

# Modelling the dynamic magneto-thermomechanical behaviour of materials using a multi-phase EOS.

Le Blanc Gaël<sup>1,3</sup>, Jacques Petit<sup>1</sup>, Pierre-Yves Chanal<sup>1</sup>, L'Eplattenier Pierre<sup>2</sup>, Avrillaud Gilles<sup>3</sup>

<sup>1</sup>Centre d'Etudes de Gramat, Gramat, France

<sup>2</sup>LSTC, Livermore, USA

<sup>3</sup>ITHPP, Thégra, France

## Summary:

For several years the "Centre d'Etudes de Gramat (CEG)" has been studying the behaviour of materials by means of experimental devices using High Pulsed Powers technologies. Among them, GEPI is a pulsed power generator devoted to ramp wave (quasi isentropic) compression experiment in the 1 GPa to 100 GPa pressure range. It may also produce non shocked high velocity flyer plates in the 0.1 km/s to 10 km/s range of velocity. The basic principle is based on a strong current circulation into electrodes. This current generates within the electrode a magnetic pressure wave (several GPa via the Laplace forces) and a strong rise of the temperature (several thousands K) due to Joule effect. Depending on that temperature, materials may be locally subjected to phase transitions such as solid to liquid or liquid to vapor.

Modelling a GEPI shot requires an Electromagnetism/Mechanical/Thermal 3D solver to study all the physical phenomena. CEG has selected LS-DYNA because a new electromagnetism solver is coupled to the historical solvers (mechanical and thermal) in LS-DYNA beta version 980. However, there is, at the moment, no equation of state with phase transitions available in LS-DYNA standard version. It is for this reason that the GRAY multi-phases EOS, developed at LLNL, is implemented as a user subroutine in LS-DYNA. The GRAY EOS allows taking into account phase transitions thanks to energies threshold.

In this paper, the GEPI device is briefly described as well as the LS-DYNA EMAG solver. The GRAY EOS is described and its implementation is discussed. Examples of applications are presented, in particular, the modelling of a GEPI experiment involving local liquefaction of the electrodes. The numerical free surface velocities are compared to experimental measurements. The liquefaction process is analyzed and compared to post-mortem observation on the electrodes. To conclude, the model limitations and potential improvements are presented.

## Keywords:

LS-DYNA, magneto hydrodynamic, multi-phase, GRAY EOS.

## 1 Introduction

For several years the “Centre d’Etudes de Gramat (CEG)” has been studying the behaviour of materials by means of experimental devices using High Pulsed Powers technologies. Among them, GEPI is a pulsed power generator devoted to ramp wave (quasi isentropic) compression experiments in the 1 GPa to 100 GPa pressure range [1][2]. It may also produce non shocked high velocity flyer plates in the 0.1 km/s to 10 km/s velocity range. The basic principle is based on a strong current circulation into electrodes. This current generates within the electrode a magnetic pressure wave (several GPa via the Laplace forces) and a strong rise of the temperature (several thousands K) due to Joule effect (see figure 1). Depending on this temperature, materials may be locally subjected to phase transitions such as solid to liquid or liquid to vapor.

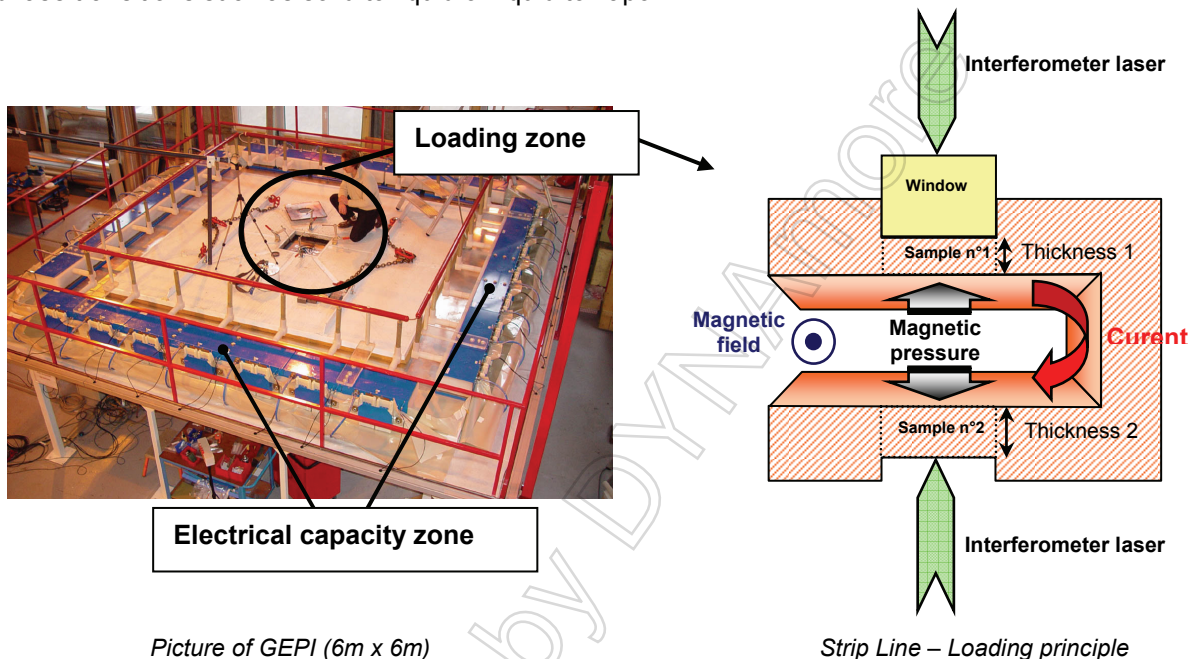


Figure 1: GEPI and loading principle.

Modelling a GEPI shot requires an Electromagnetism/Mechanical/Thermal 3D solver as LS-DYNA to study all the physical phenomena [3][4][5]. However, LS-DYNA standard version does not have any mechanical equation of state with phase transitions. On the other hand, the user EOS implementation is available [6][7]. Hence, this solution has been selected. The model selected is the GRAY EOS [8][9] developed at the LLNL because it is adapted to simulate effects of rapid energy deposition like GEPI shot.

The study is divided in three main parts. In the first one, the LS-DYNA electromagnetic solver is briefly described. In the second one, the GRAY EOS and its implementation in LS-DYNA are presented. The last part presents an application to a particular GEPI shot.

## 2 The LS-DYNA electromagnetic solver

A new electromagnetism module is being developed in LS-DYNA for coupled mechanical/thermal/electromagnetic simulations [10][11]. One of the main applications of this module is Electromagnetic Metal Forming but other magneto hydrodynamic processes could be simulated. The electromagnetic fields are computed by solving the Maxwell equations in the eddy-current approximation. These equations are solved using a Finite Element Method (FEM) for the conductors coupled with a Boundary Element Method (BEM) for the surrounding air/insulators. Both methods use elements based on discrete differential forms (Nedelec-Like elements) for improved accuracy.

## 2.1 Maxwell equations

The Maxwell equations are recalled here:

$$\vec{\nabla} \wedge \vec{E} = -\frac{\partial \vec{B}}{\partial t} \quad (1)$$

$$\vec{\nabla} \wedge \frac{\vec{B}}{\mu} = \vec{j} + \varepsilon \frac{\partial \vec{E}}{\partial t} \quad (2)$$

$$\nabla \bullet \vec{B} = 0 \quad (3)$$

$$\nabla \bullet \varepsilon \vec{E} = 0 \quad (4)$$

$$\nabla \bullet \vec{j} = 0 \quad (5)$$

$$\vec{j} = \sigma \vec{E} + \vec{j}_s \quad (6)$$

Where  $\sigma$  is the electrical conductivity,  $\varepsilon$  is the permittivity,  $\mu$  is the permeability,  $\vec{E}$  is the electric field,  $\vec{B}$  the magnetic flux density,  $\vec{j}$  the total current density, and  $\vec{j}_s$  is a source current density. We solve

Maxwell's equations under eddy-current approximation [11]:  $\varepsilon \cdot \frac{\partial \vec{E}}{\partial t} \ll \sigma \cdot \vec{E}$ . We thus neglect the second term of the right hand side of equation (2). These equations are solved using magnetic vector potential and electrical scalar potential.

## 2.2 Finite element method for conductors and Boundary Element Method for air or insulator

The FEM method solving Maxwell equations in conductor use a library called "FEMSTER". This library has been developed at the Lawrence Livermore National Laboratories. FEMSTER provides discrete numerical operator as the exterior derivatives gradient, curl and divergence and also the div-grad, curl-curl and grad-div. The FEMSTER library has especially two main advantages. They define spaces with an exact representation in the De-Rham sequence and they also exactly satisfy numerically relations like  $\text{curl}(\text{grad})=0$  or  $\text{div}(\text{curl})=0$ . This is very important for conservation laws during resolution.

The BEM method uses an intermediate variable, "surface current". This new variable is introduced on the boundary between conductor and insulator so as to produce the same magnetic field in the insulator region as the magnetic field created by the actual volume current flowing through the conductor. The BEM method is very appealing since it does not need a mesh in the air surrounding the conductor. It thus avoids the meshing problems associated with the air mesh like complicated conductor geometries; small gaps that generating very small and distorted elements and so forth. Furthermore, this approach avoids remeshing problems when the conductors are moving, which results in large air mesh distortion. On the other hand the main BEM drawback is the machine cost especially high memory requirement as well as longer CPU time to assemble the matrices because this method generates full dense matrices in place of the sparse FEM matrices.

## 2.3 Coupling with LS-DYNA

The electromagnetic module developed is coupled with the historical LS-DYNA solvers, the mechanical and thermal ones.

Once the magnetic field and current density, respectively  $\vec{B}$  and  $\vec{j}$ , have been computed, the Laplace force,  $\vec{F} = \vec{j} \wedge \vec{B}$ , is evaluated and added to the mechanical solver as a nodal force. The electromagnetic and mechanical solvers each have their own time step. The mechanical one is about ten times smaller than the electromagnetic one for these kinds of applications. The mechanical module computes the conductor deformations and the new geometry which is then used to compute the electromagnetic fields in a Lagrangian way.

The thermal coupling is necessary because a flowing current in a non perfect conductor generates Joule heating and thus a temperature rise. The material behaviour is often temperature dependent

especially the electrical conductivity. The joule heating power,  $\frac{j^2}{\sigma}$ , is added to the thermal solver

allowing to update the temperature. Furthermore, the Joule heating associated with high pressure (about 10 GPa) drives the material into phase transition from solid to liquid or liquid to vapor.

Unfortunately, there is no mechanical equation of state with phase change like GRAY EOS in the standard LS-DYNA version. Nevertheless, it is possible to implement this kind of EOS using the user option available in LS-DYNA.

### 3 The GRAY EOS and its implementation in LS-DYNA

The GRAY EOS was developed by Grover, Royce, Alder and Young at the Lawrence Livermore National Laboratory in the seventies. This multi phases EOS for metals has been developed to compute the effects of rapid energy deposition in a variety of high speed phenomena such as the deposition of X-ray energy, exploding wires or explosive compression of magnetic flux. At first, the GRAY EOS is briefly described then its implementation in LS-DYNA is presented.

#### 3.1 GRAY EOS principle

The goal of this part is a concise GRAY EOS description. Further details are presented by Royce in [8]. First, the main hypotheses are recalled:

- Entropy of melting is a constant
- The temperature is computed via the specific heat associated with each phase.
- The melting temperature is computed via the Lindemann Law.
- The liquid-vapor phase is described by a Van Der Waals model.

For each phase, the generic form of the temperature and the pressure are defined below:

$$\begin{aligned} T &= f_{\alpha}(v, E) \\ P &= P_1(v, E) + P_c^{\alpha}(v, T) + P_{cc} \end{aligned} \quad (7)$$

Where :

- $T$ , temperature
- $f_{\alpha}$ , function defining the temperature in  $\alpha$  phase ( $\alpha$ =solid, melting, liquid or vapor).
- $E$ , internal energy
- $v$ , specific volume
- $P_1$ , Pressure computed via linear Gruneisen law
- $P_c^{\alpha}$ , temperature dependent corrected pressure for the  $\alpha$  phase
- $P_{cc}$ , additional term to take account initials conditions

All these terms have been described in details in [8] thus only the energies phase transition criteria are given here in table 1.

Table 1: GRAY EOS – phase transition criteria [8].

Solid Phase	Liquid Phases			Vapor Phase
$E \leq E_{melt}$	Melting solid/liquid	Liquid	Hot Liquid	$v < v_j$
	$E_{melt} \leq E \leq E_{liq}$	$E_{liq} \leq E \leq E_{hot\_liquid}$	$E_{hot\_liquid} \leq E$	

### 3.2 GRAY EOS implementation in LS-DYNA

User equations of state are available in LS-DYNA version 971. The user must make his own LS-DYNA compilation using object files given by LSTC. The principle is described figure 1.

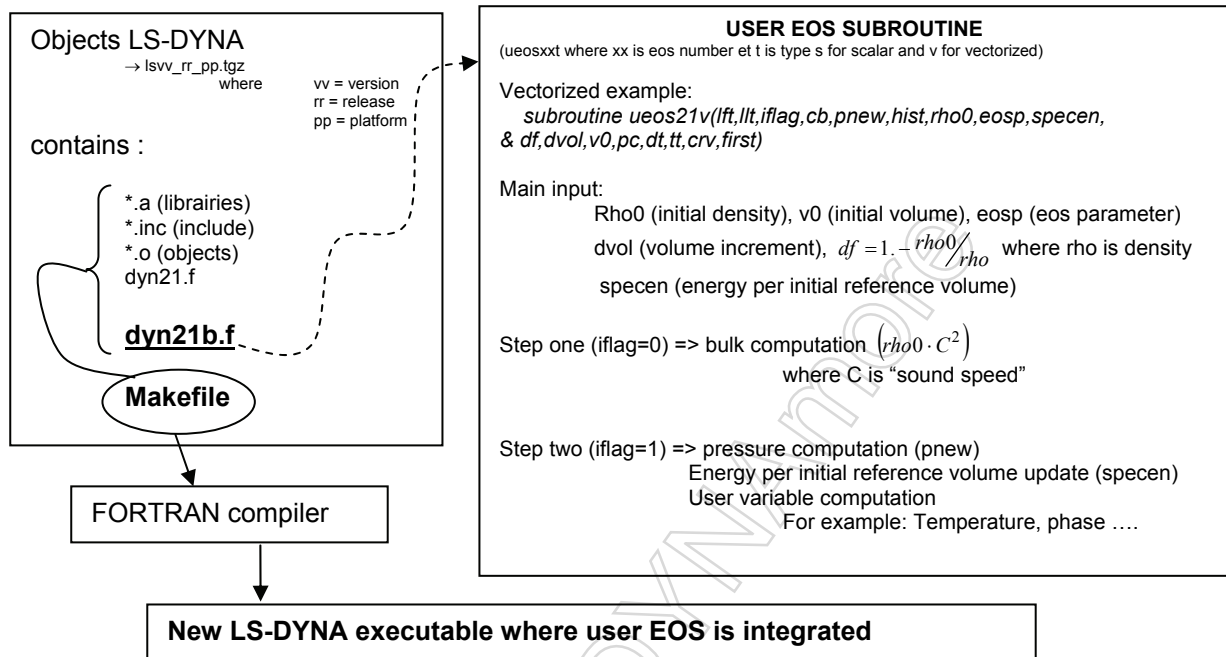


Figure 2: User equation of state implementation in LS-DYNA.

The GRAY EOS implementation has been realized in three main steps. At first step, the EOS presented by Royce in [8] has been faithfully implemented in LS-DYNA mechanical only. The second step consists in implementing GRAY EOS in LS-DYNA 980 beta version with electromagnetism. The main task is the coupling with the electrical model available in LS-DYNA 980 (the Burgess model [12]). The electrical Burgess model has been developed at Sandia National Laboratories. It is inspired from the Kidder model. It describes the temperature and density dependence of the electrical conductivity. The phase transitions are taken into account. The solid to liquid transition depends on a temperature criteria and the vaporization occurs immediately in expansion. The generic resistivity expression is (further details in [12]):

$$\eta = \eta_{\alpha}(T, v) \quad (8)$$

Where:

$\eta$ , electrical resistivity

T, temperature

$\eta_{\alpha}$ , function defining the resistivity in  $\alpha$  phase ( $\alpha$ =solid, liquid or vapor).

v, specific volume

The coupled GRAY/BURGESS method is based on the additional "user common". It is presented in the diagram of figure 3.

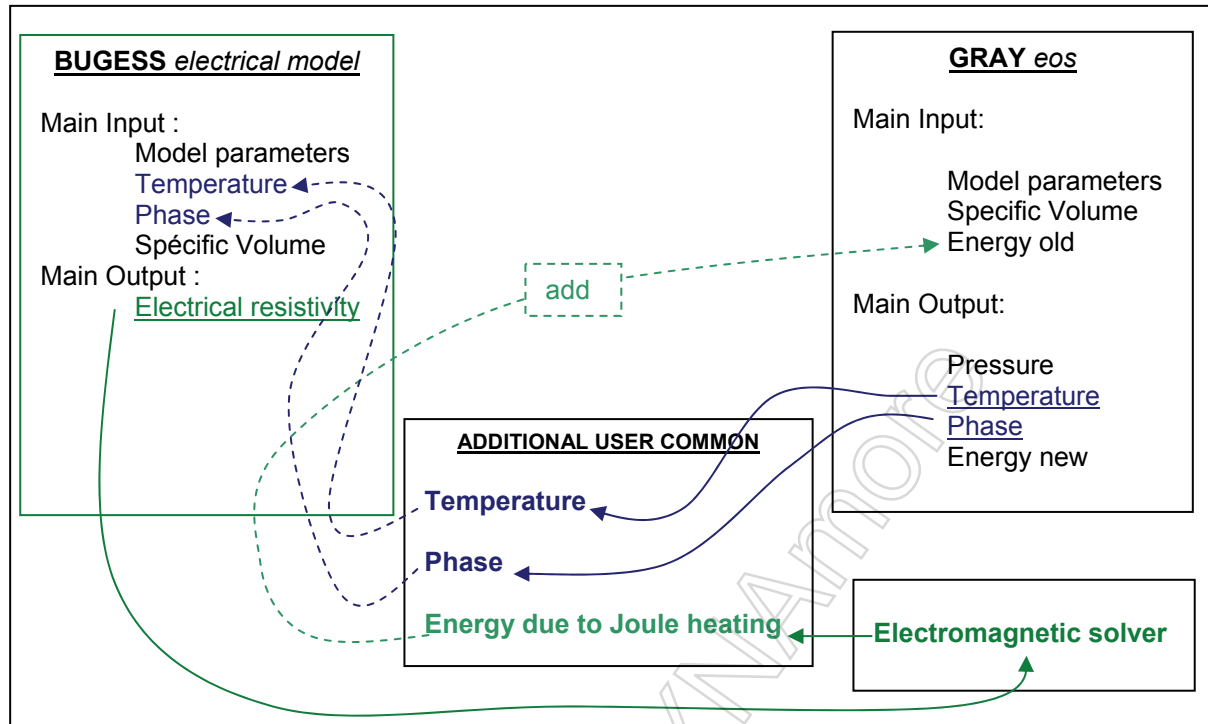


Figure 3: Coupling between the GRAY EOS and the Burgess electrical model – LS-DYNA 980 beta.

The third step consists in implementing a few improvements. At first, a discontinuity appears during the liquid/vapor transition. This is shown figure 4. To smooth down this jump, an empirical model has been implemented in the equation of state. This modification acts on the GRAY variable defining the attractive potential for vapor ( $A_y$  in [8]). At the moment the  $A_y$  variable is temperature dependent.

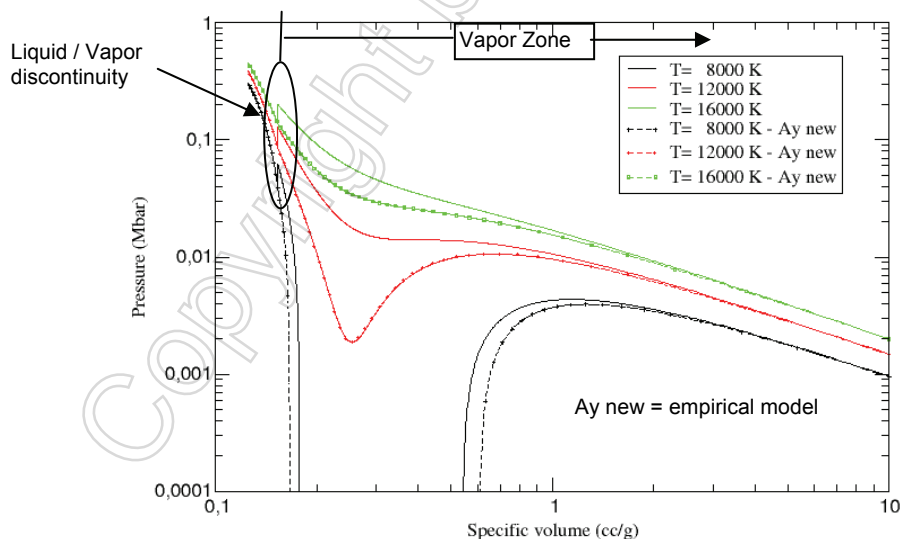


Figure 4: Discontinuity at liquid to vapor transition – Copper.

Then, the improvement proposed by Young in [13] around the transition liquid/vapor at low pressure has been also implemented. This model is briefly presented in figure 5.

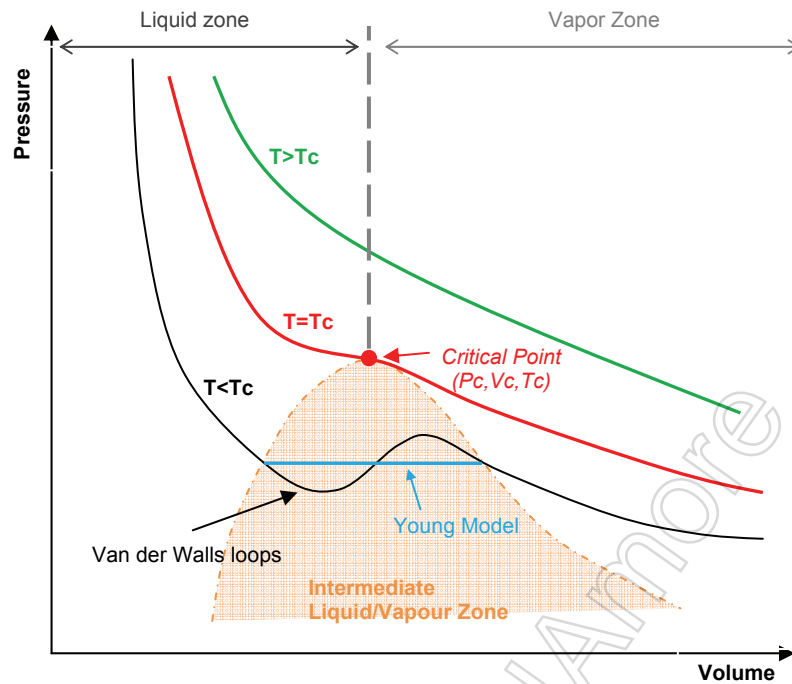


Figure 5: New phase = Liquid/Vapor transition at low pressure – Young's Model [13].

The Van der Waals loops deletion is important because it allows avoiding large problems such as negative sound speeds. The implementation of this intermediate phase is inspired from the algorithm used in PUFF8 [9]. For each material, the critical dome is computed first then it is implemented in the EOS as parameter. At each cycle, a checking step is realized in each cell to determine if the cell is in the Intermediate Liquid/Vapor Zone.

## 4 GRAY EOS applications

### 4.1 Experimental configuration and results

The experimental configuration is presented figure 6. The strip line is described here.

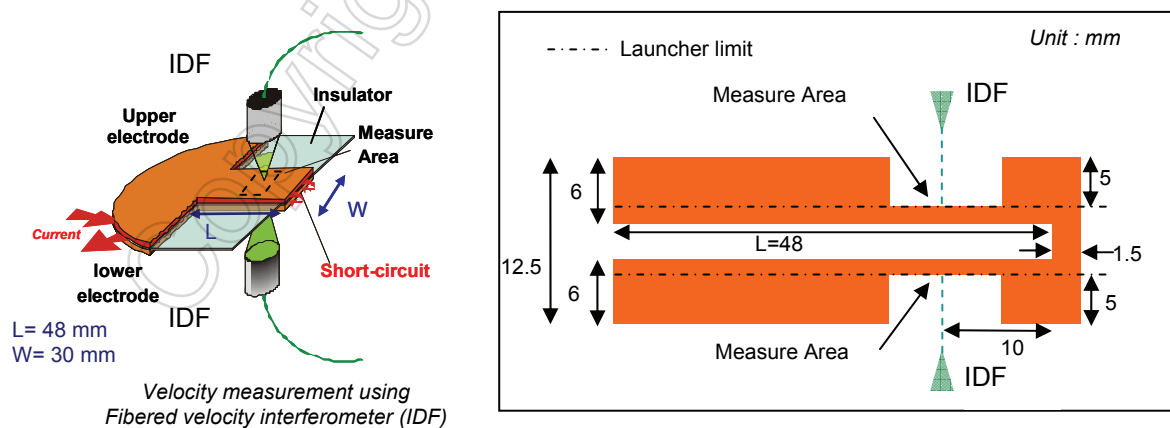


Figure 6 : GEPI shot 475 – experiment setting [5].

The average current (12 measurement points via MCCI technologies [5]) is presented in Figure 7 and is in agreement with another current measurement from a Rogowsky coil. Interferometer free surface velocity measurements are also shown on Figure 7 [14].

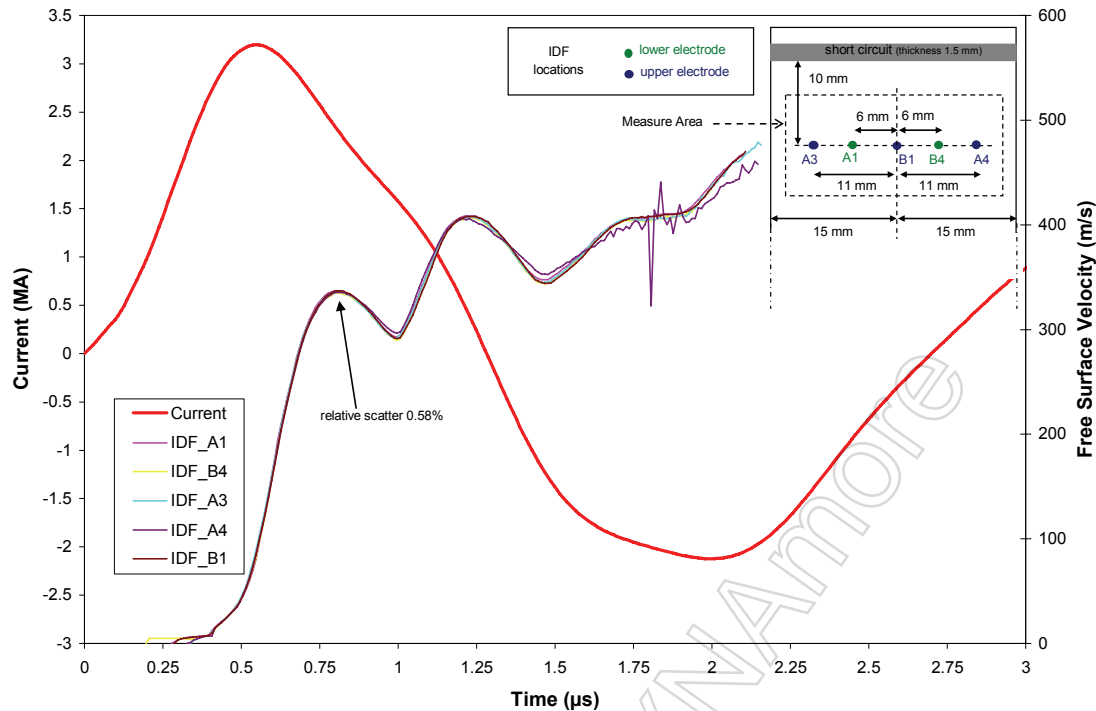


Figure 7: GEPI shot 475 – experimental measured – current and free surface velocities [5].

The free surface velocities are very homogeneous, representing a great improvement compared to an older design. The relative scatter is lower than 0.6%. These scatters are measured close to the short circuit and near the edges. Hence, the magnetic pressure is very homogeneous, in the transversal direction, at 10 mm from short circuit.

#### 4.2 Numerical model

In order to limit the memory requirement of the Electromagnetism module, only the launcher (see figure 8) is modelled with a relatively fine mesh. It was not possible to model the whole circular part due to the large number of cells and because for the moment, only a homogeneous current can be injected at the boundaries in LS-DYNA. The experimental current is injected at the straight entrance of the 1 mm thick launcher. The rest of the electrodes are modelled using only the mechanical solver (see Figure 10). It means that the electromagnetic effects are taken into account only in the launcher. This should not influence the distribution of the magnetic pressure except near the lateral edges and the RAM cost become acceptable (about 8 to 10 Go) with a relative fine mesh (see Figure 8). The mesh is composed of 185 592 bricks elements with 15 elements through the thickness of the launcher (2 in the initial skin depth (about 0.1 mm) which tends to grow quickly with the rise of the electrode temperature and then 13 for the rest of the electrode with a ratio). This seems sufficient to correctly handle the magnetic diffusion as demonstrated in [10]. The update of the electromagnetism matrices is necessary because a strong mesh deformation occurs. This update takes place each 5 and 20 electromagnetic cycles for the FEM and BEM matrices respectively.



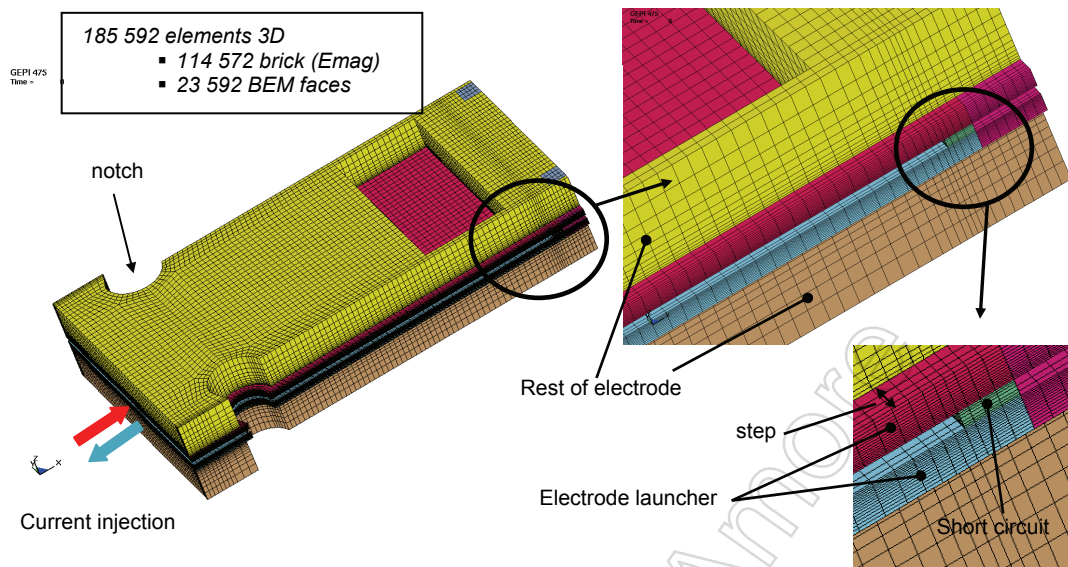


Figure 8 : LS-DYNA GEPI shot 475 – Numerical model.

A coupled mechanical / thermal / electromagnetism simulation has been performed. The electrical conductivity versus temperature and density is computed using a Burgess equation of state (where the conductivity is temperature dependent and the phase changes are taken into account). For the mechanical response, the Johnson-Cook model [14] (\*MAT\_15) coupled with the user equation of state GRAY was chosen. The temperature and phase transition are computed in GRAY then sent to Burgess to update the electrical conductivity (see § 3). The thermal conduction is not taken into account here because thermal propagation is very slow compared to the Ohm heating process (few  $\mu$ s). The temperature rise is driven by the Joule heating.

The validation of the GRAY implementation was realized by free surface velocities comparison between LS-DYNA standard modelling, UNIDIM modelling and experimental results (see figure 9). UNIDIM is a one dimensional magneto hydrodynamic code developed at CEG [15].

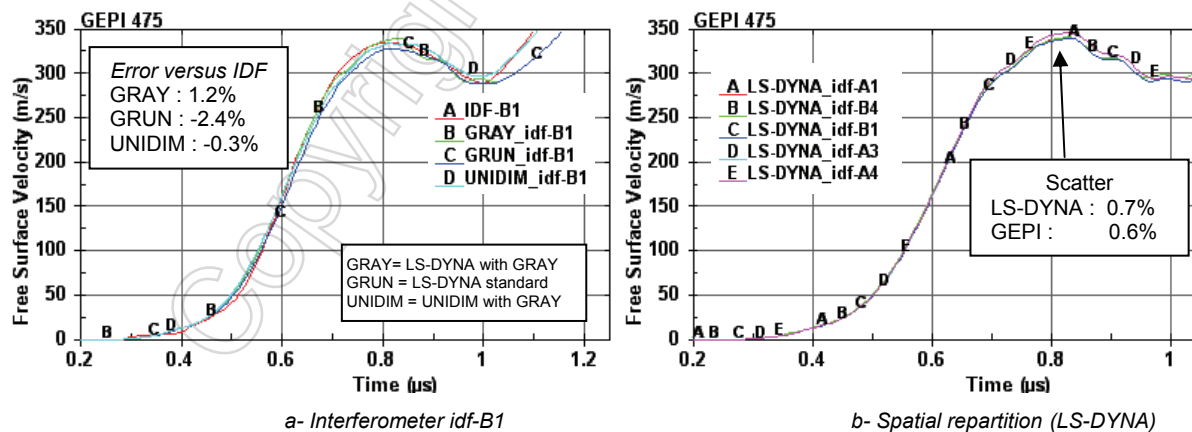


Figure 9 : GEPI shot 475- copper, W=30 mm, thick=1 mm – Free surface velocities.

The LS-DYNA simulations are done using the experimental current without any correction factor. The numerical velocities are close to the experimental ones. Using GRAY improves lightly the prediction compared to the standard modelling. The UNIDIM model is close to the LS-DYNA model: GRAY EOS coupled to Burgess electrical and Johnson-Cook laws are also used in UNIDIM. A coefficient, about 0.95, is applied to the current to represent the edge effects in UNIDIM [16]. On the other hand the standard LS-DYNA modelling is based on the coupling option available in LS-DYNA. In the standard LS-DYNA modelling, the thermal, mechanical and electromagnetic solvers are used. The material models used here are: Johnson-Cook and Gruneisen EOS, Burgess coupled to thermal linear model.

The main advantage of GRAY EOS is the knowledge of the material state and more realistic temperature estimation during the simulations. The historical temperature profiles comparison between GRAY and standard modelling is presented figure 10. The phase transition is also described on figure 10 (solid = 1, solid/liquid melting = 2, liquid = 3, hot liquid = 4, liquid/vapour = 5, vapour  $\geq 6$ ).

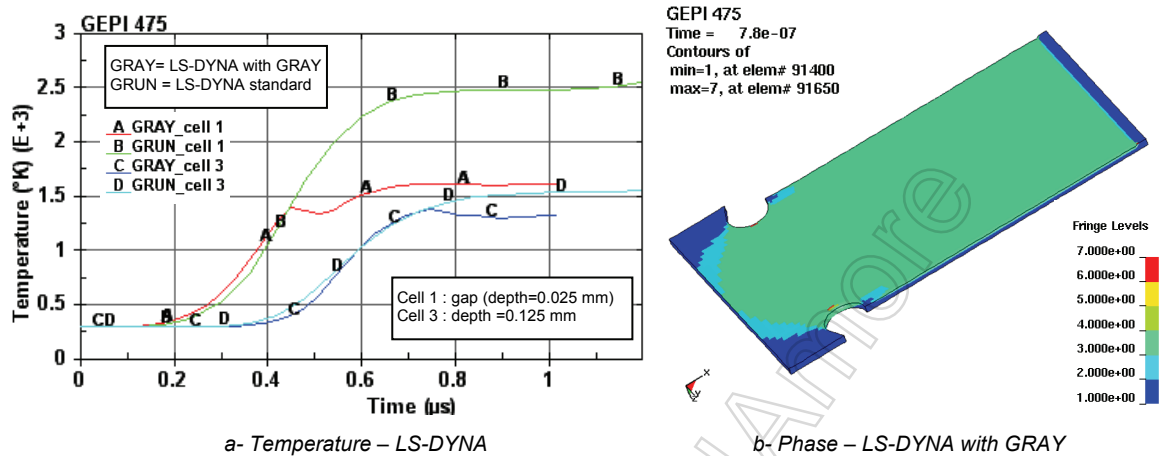


Figure 10: LS-DYNA GEPI shot 475 – Temperature and phase transition.

Having access to these kinds of variable could be very important for high speed flyer analysis in order to define the real characteristics at impact (state of the impactor).

Nevertheless, using GRAY EOS with a Lagrangian approach without adaptive mesh or erosion is limited because local vaporization involves large expansion. It results in large mesh deformation. These distortions could stop the computation because the electromagnetic solver convergence becomes very difficult in particular for the BEM or “negative volume error”. Indeed the electromagnetic convergence is impossible when two neighbour faces have too different aspect ratios. (The EM BEM solver cannot deal with triangular faces yet). This kind of problem is presented figure 11.

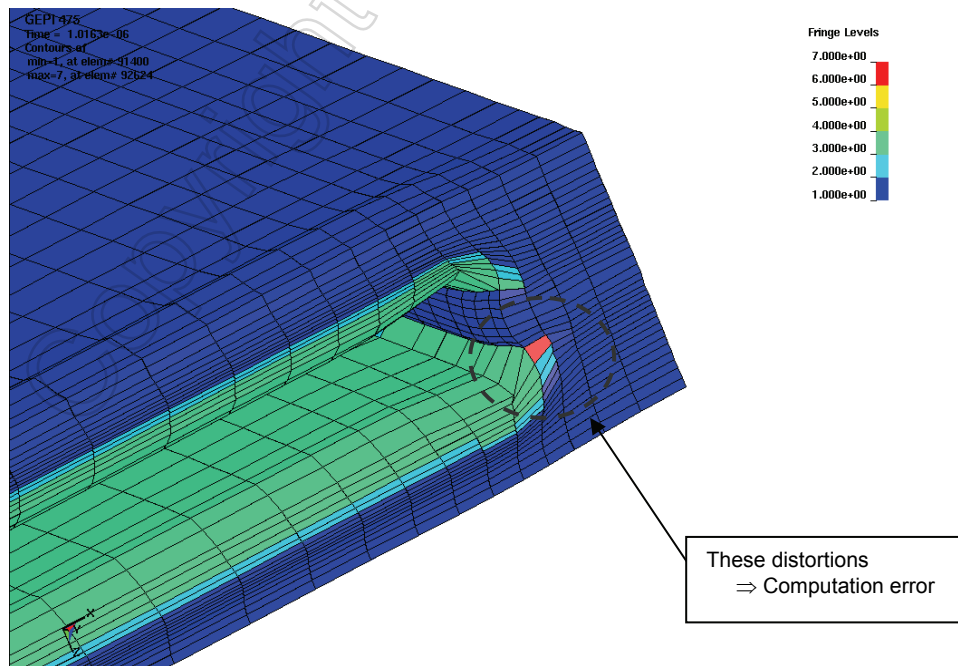


Figure 11: LS-DYNA GEPI shot 475 - Phase – mesh distortion problem close to the short circuit.

## 5 Conclusion

The User EOS option available in LS-DYNA is a good tool to understand complex coupled mechanisms, such as phase transitions. The GRAY EOS implementation seems correct for two main reasons.

First, the numerical velocities reproduce rather correctly the GEPI experimental measurements. Nevertheless, phase transitions have a little effect on free surface velocity compared to magnetic pressure loading. Indeed, free surface velocities computed with Gruneisen EOS are also good.

Then the post mortem analysis of an old GEPI shot close to the shot 475 (current and electrode geometry) shows a fusion thickness about 27%. UNIDIM modeling seems valid because the computed fusion thickness at 2.4  $\mu\text{s}$  is 22%. LS-DYNA modeling is stopped at 1  $\mu\text{s}$  (see figure 11), it's so soon to compare the computed fusion thickness to the post mortem experimental one. The Joule heating is not finished at this time. Nevertheless, the comparison is possible with UNIDIM at 800 ns. LS-DYNA computes 10-15% fusion thickness versus 6% for UNIDIM. The UNIDIM result is lower than the LS-DYNA one because the mesh is finer (100 cells in the launcher versus 15 in LS-DYNA). Hence the fusion thickness computed by LS-DYNA is overestimated here. A finer mesh seems necessary to improve LS-DYNA accuracy. This will become possible with the future MPP version. More comparisons with experimental results will also help improving the 3D modeling (for example: aluminum strip line with smaller width using for flyer application).

The main problem of the model is the loss of convergence due to mesh distortion in vapor or liquid phases. It is inherent to a Lagrangian approach. An alternative solution consists in remeshing options and/or erosion but it isn't available in LS-DYNA for the electromagnetic solver yet. Furthermore, adaptive meshing would probably involve an increase in the cell number and the memory required then CPU time could increase a lot. Hence, a prior step must be realized before remeshing option. It's the electromagnetic solver parallelization. This step is actually being examined at LSTC and an MPP version of the electromagnetic solver should soon be available.

A kind of "cavitation model" has been implemented in UNIDIM. It consists in void insertion as soon as the liquid pressure is lower than the pressure cutoff. In this case, a null pressure is imposed in the liquid then volume and energy cell are updated in order to avoid incoherent state. The cavitation model allows improving the accuracy after the second velocity peak (see figure 12). Indeed, void insertion close to the gap changes the Laplace Force effect because the matter is discontinuous and the third velocity bounce is lowered.

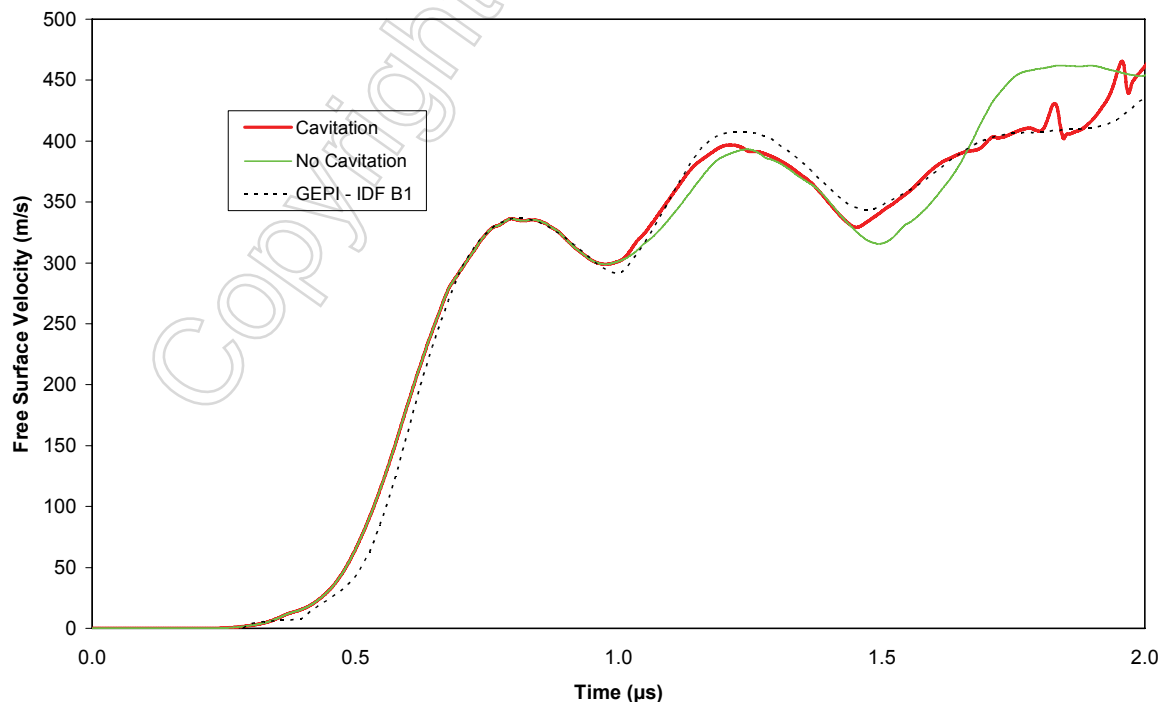


Figure 12 : UNIDIM – cavitation in liquid phase - GEPI shot 475 – Free surface velocities IDF B1.

## 6 References

- [1] Hérelil P.L, Lassalle F. and Avrillaud G.: " GEPI : An ICE Generator for Dynamic Material characterization and Hypervelocity Impact", Shock Compression of Condensed Matter - 2003.
- [2] Hérelil P.L and Avrillaud G.: "GEPI : an ICE generator for dynamic material studies", Presentation for the 55th Meeting of the Aeroballistic Range Association (ARA), Freiburg, Germany, September 27-October 1, 2004.
- [3] L'Eplattenier P.: "LS-DYNA<sup>®</sup> keyword user's manual for electromagnetic solver", LSTC, not printed.
- [4] Lefrançois A., L'Eplattenier P. and Burger M.: "UCRL-TR-219179 - Isentropic Compression in a Strip Line, Numerical Simulation and Comparison with GEPI Shot 268", Lawrence Livermore National Laboratory, February 2006.
- [5] Le Blanc G, Chanal P.Y., L'Eplattenier P, Avrillaud G.: " Ramp wave compression in a copper strip line: comparison between MHD numerical simulations (LS-DYNA<sup>®</sup>) and experimental results (GEPI device) – CEG, LSTC, ITHPP – 10<sup>th</sup> LS-DYNA international conference 2008.
- [6] Hallquist J.O.: "LS-DYNA<sup>®</sup> theory manual", LSTC, March, 2006.
- [7] LSTC: "LS-DYNA<sup>®</sup> keyword user's manual", LSTC, May, 2007.
- [8] Royce E.B: "UCRL-51121 - GRAY, A THREE-PHASE EQUATION OF STATE FOR METALS", LLNL, September 3, 1971.
- [9] Seaman L: "SRI PUFF 8 computer program for one dimensional stress wave propagation", SRI, August, 1978.
- [10] L'Eplattenier P., Cook G., Ashcraft C., Burger M., Shapiro A., Daehn G. and Seth M.: "Introduction of an Electromagnetism Module in LS-DYNA for Coupled Mechanical-Thermal-Electromagnetic Simulations", 9<sup>th</sup> International LS-DYNA Users Conference – 2004.
- [11] L'Eplattenier P., Cook G., Ashcraft C.: "Introduction of an electromagnetism module in LS-DYNA for Coupled Mechanical Thermal Electromagnetic Simulations", LSTC, 3<sup>rd</sup> ICHSF, 2008.
- [12] Burgess T.J.: "Electrical resistivity model of metals", 4<sup>th</sup> International Conference on Megagauss Magnetic-Field Generation and Related Topics, Santa Fe, NM, USA, 1986.
- [13] Young D.A: "UCRL-51575 – Modification of the GRAY equation of state in the liquid-vapor region", LLNL, April 15, 1974.
- [14] Chanal P.Y. and Luc J.: "Innovative laser interferometer's development and metrology for material behaviour studies", 14<sup>ème</sup> Congrès International de Métrologie, Paris, Juin 2009.
- [15] Johnson G.R, Cook W.H: "Fracture characteristics of three metals subjected to various strains, strain rates, temperatures and pressures", Engineering Fracture Mechanics vol 21 n°1 page 31-48, 1985.
- [16] Petit J: "adaptation du code UNIDIM au cas de rampe de pression magnétique sur ligne plate – Application à un cas test", CEG Internal report n°2002-00009/CEG/NC, 2002.
- [17] Knoepfel H.: "Pulsed High Magnetic Fields" – NHPC – 1970.